5th ECPMG Delft · 2024

Proceedings of the 5th ECPMG 2024
5th European Conference on Physical Modelling in Geotechnics
2-4 October 2024, Delft, the Netherlands

Evaluating the Impact of Overburden Pressure on Liquefaction Susceptibility in Granular Soils: Insights from Centrifuge Modeling

T. Abdoun
New York University Abu Dhabi, Abu Dhabi, U.A.E., tarek.abdoun@nyu.edu

M. Ni
Amazon Development Center, Seattle, U.S.A., niminly2008@gmail.com

M.E. Ghazy
New York University Abu Dhabi, Abu Dhabi, U.A.E., meg9874@nyu.edu
Arab Academy for Science, Technology and Maritime Transport (AASTMT), Alexandria, Egypt

W. El-Sekelly
New York University Abu Dhabi, Abu Dhabi, U.A.E., we20@nyu.edu
Dept. of Structural Eng., Mansoura University, Mansoura, Egypt

ABSTRACT: This study presents an investigation of overburden pressure effect on liquefaction triggering of liquefiable granular deposits. Six centrifuge experiments were performed on idealized field cases with varying relative densities, boundary conditions, and overburden pressures. The simulations included cyclic loading applied at the base of a 5-m deposit of the soil. Acceleration, excess pore pressure during and after shaking, shear stress ratio, and shear strain time histories were identified at multiple locations in the soil deposit. The analysis of experimental recordings revealed significant effects of overburden pressure on the liquefaction responses of clean Ottawa sand. It was found that sand under high overburden experiences more partial drainage during and after shaking. The results showed stress-based correction factors field K_σ values larger than 1.0 inconsistent with the traditional approach of obtaining (K_σ) from undrained laboratory tests. This discrepancy was attributed to the partial drainage conditions simulated in both single and double drainage setups. Overall, this study provides valuable insights into the behavior of saturated soils under high overburden pressures, which can help engineers make more accurate and reliable liquefaction potential assessments.

1 INTRODUCTION

Liquefaction-induced soil failure presents a significant challenge in the field of geotechnical earthquake engineering. The primary methodology employed for assessing liquefaction triggering is the Simplified Method, initially introduced by Seed and Idriss (1971). This approach uses field charts that have been calibrated using historical instances of both liquefaction occurrences and non-occurrences. The soil's liquefaction resistance, or cyclic resistance ratio (CRR), is determined by correlating it with field measurements obtained from standard penetration tests (SPT), cone penetration tests (CPT), and in situ measurements of shear-wave velocity (V_s).

These charts are primarily calibrated based on effective overburden pressure (σ'_{v0}) values below 2 atmospheres (≈ 200 kPa) (Dobry and Abdoun 2015). As a result, they may not be suitable for projects that involve higher pressures, such as sand foundation layers under large dams and embankments, which can reach 6, 8, or even over 10 atmospheres (Gillette, 2013). Accurate evaluation of liquefaction resistance is critical for such loads due to the potential consequences of failure and the high cost of designing and retrofitting against liquefaction.

Seed (1983) pointed out that the CRR measured in undrained cyclic stress-controlled laboratory tests decreases as the effective confining pressure increases. To account for this, he proposed a correction factor, $K_\sigma < 1$, that multiplies the CRR obtained from the chart to produce a smaller field CRR valid for the high confining pressures encountered in or under embankment dams. This factor is defined as:

$$K_\sigma = (CRR)_{\sigma'_{v0}} / (CRR)_1 \quad (1)$$

where $(CRR)_{\sigma'_{v0}}$ and $(CRR)_1$ represent cyclic resistance ratios in the critical liquefiable layer under $\sigma'_{v0} > 1$ atm and $\sigma'_{v0} = 1$ atm, respectively.

Researchers have investigated the correlation between K_σ and vertical overburden pressure (σ'_{v0}) over the past few decades, typically using undrained cyclic laboratory tests (Seed 1983; Harder 1988; Seed and Harder 1990; Vaid and Thomas 1995; Vaid and Sivathayalan 1996; Hynes et al. 1999; Youd, et al. 2001; Boulanger 2003; Boulanger and Idriss 2004; Idriss and Boulanger 2008; Montgomery, et al. 2012; Dobry and Abdoun 2015). The current State of Practice (SoP) largely follows the recommendations of Youd, et al. (2001) and Idriss and Boulanger (2008). Youd, et al. (2001) analyzed available data and adopted the following expression: $K_\sigma = (\sigma'_{v0}/P_a)^{f-1}$, where P_a is atmospheric pressure. The exponent f ranges from 0.7-0.8 for relative density (D_r) of 40%-60% and 0.6-0.7 for D_r of 60%-80%. Boulanger (2003) and Idriss and Boulanger (2008) re-evaluated the effect of overburden pressure on cyclic resistance ratio using a critical state framework. Depending on the relative density, the recommended K_σ values from these two studies for $\sigma'_{v0} = 6$ atm range between 0.5 and 0.85.

2 CENTRIFUGE EXPERIMENTS

The accuracy of K_σ results obtained from undrained cyclic testing is still a topic of debate in geotechnical engineering. The main criticism of the state of practice is that it provides a wide range of values and is based on undrained small-scale testing. It was observed that liquefaction may not be fully undrained but rather partially drained. Therefore, dynamic centrifuge modeling was utilized to examine the effect of field drainage conditions on the K_σ factor. The K_σ effect under single and double drainage conditions was investigated by Ni et al. (2020; 2021) and Abdoun et al., (2020) through a series of centrifuge experiments modelled using one-dimensional (1D) stacked ring laminar container. Herein, the results of six of these centrifuge experiments are presented.

In the centrifuge experiments performed on idealized field cases, multiple parameters were adjusted, such as overburden pressures, relative densities (D_r) and boundary conditions. Table 1 provides a summary of each test, detailing the respective values of overburden pressures, relative densities, gravitational acceleration level and stating the boundary conditions. The position of various sensors, including accelerometers, pore pressure transducers, vertical LVDTs, and bender elements, within the experimental setup used for both single and double drainage scenarios is shown in Figure 1. The model is comprised of a 5-meter layer of dry pluviated, saturated clean sand, overlaid by a layer of rounded granulated lead particles, of variable thickness. The inclusion of lead grains served two purposes: to generate the desired level of inertially-generated shear stresses during shaking, and to provide the necessary vertical effective overburden pressure due to its high dry unit weight of 62.6 kN/m^3. To prevent the lead grains from sinking into the saturated sand, a transition layer was introduced between the lead grains and the sand layer, acting as a filter.

Furthermore, to maintain the fluid flow characteristics of the sand at 1 g, the dry pluviated sand was saturated using a viscous fluid, with the viscosity adjusted based on the g level using viscous fluid. In the case of the double drainage model, Geocomposite and Geonet strips were added to facilitate drainage from the base of the model. For more detailed information on the construction and saturation of the models, Ni et al. (2020) can be referred to, while Ni et al. (2021) provides additional details specifically related to the double drainage model.

For this project, the centrifuge models underwent a 1D shaking event by the centrifuge in-flight shaker applied at the base. The input motion used for all shakings was a 10-cycle uniform sinusoidal signal with a prototype frequency of 2 Hz. The amplitude of each input motion was selected to achieve a degree of liquefaction (r_u) of ~0.8, which was considered the failure criterion for this study.

In order to calculate the values of field K_σ (obtained from centrifuge tests), the centrifuge Cyclic Stress Ratio (CSR) values were obtained through the use of System Identification (SI) analysis developed by Elgamal et al. (1995; 1996) and Zeghal et al. (1995). The CSR interpreted as $CRRs$ associated with a failure criterion of $(r_u)_{max} = 0.8$. The CRR values for the $6\,atm$ and $1\,atm$ were used to calculate the field K_σ by substituting in Equation 1.

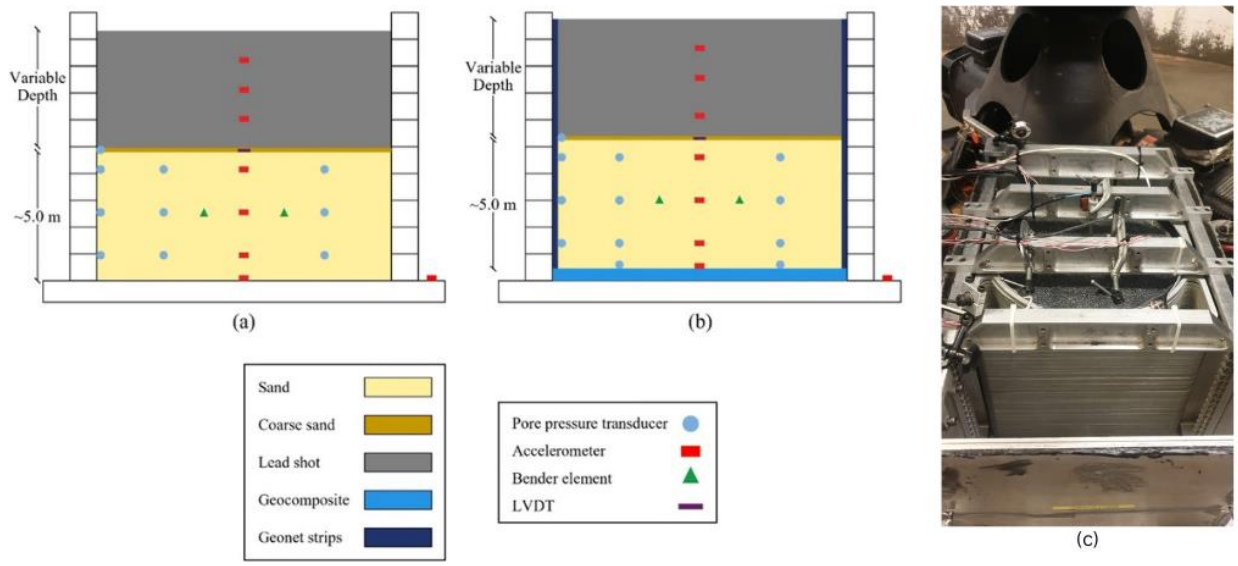

Figure 1. Configurations of Centrifuge Model Setups for (a) Single drainage tests; (b) Double drainage tests, and (c) photo for the model on the centrifuge before spinning

Table 1. Key characteristics of centrifuge experiments.

Experiment	Effective Overburden Pressrure (σ'_{v0}) (atm)	Relative Denisty (D_r) (%)	Centrifugal g-level (g)	Boundary Conditions
Test 45-1	1	45	20	Single Drainage
Test 45-6	6	45	60	Single Drainage
Test 80-1	1	80	20	Single Drainage
Test 80-6	6	80	60	Single Drainage
Test 45-1 (DD)	1	45	20	Double Drainage
Test 45-6 (DD)	6	45	45	Double Drainage

3 RESULTS

The results section primarily examines the excess pore pressure ratio and the field K_σ calculations and analyses. Figure 2 shows the time histories for the excess pore pressure ratio (r_u) for single drainage tests (Test 45-1, Test 45-6, Test 80-1, and Test 80-6). According to the figure it can be inferred that:

- (r_u) consistently showed higher values at deeper levels, with the maximum pore pressure ratio of the entire experiment, $(r_u)_{max}$, always occurring at the sensor nearest to the base of the container.
- For all four curves, peak values emerged sooner during the shaking process at shallower depths, with peaks at the lower end of the layer generally appearing towards or at the conclusion of the shaking period ($t \approx 5\ s$). In other words, the onset of dissipation began earlier at shallower depths closer to the top drainage boundary, marked by the transition and lead shot layers, and significantly later in the shaking cycle, or even after it had ended, at deeper locations distant from that boundary. The earliest peak occurrences, around 1–2 seconds, indicating the quickest commencement of dissipation, were observed at the most shallow depths and in the experiments conducted at 6 atmospheres of pressure.

Figure 3 illustrates the time histories of the shear stress ratio, determined using SI technique. The figure reveals that the stress ratios for the tests conducted at 6 atm (Tests 45-6 and 80-6) consistently exceed those from the 1 atm tests (Tests 45-1 and 80-1), suggesting that the field K_σ values are greater than 1. The cyclic resistance ratio (CRR) for each test was derived from its respective shear stress ratio, and the field K_σ values were then calculated using Equation 1. These values are documented in Table 2.

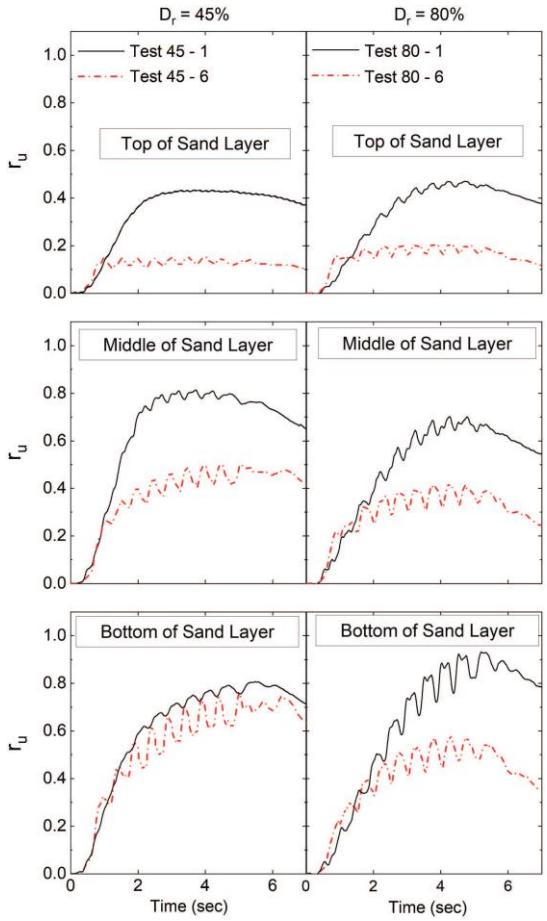

Figure 2: Time histories of excess pore pressure ratio for (a) Tests 45-1 and 45-6; and (b) Tests 80-1 and 80-6. (Ni et al. (2020))

Table 2 displays the final calculations of field K_σ, which were found to be 1.28 and 1.15 for the single drainage, for $D_r = 45\%$ and $D_r = 80\%$, respectively. The K_σ, for the double drainage tests, was found to be 1.30. The laboratory undrained K_σ obtained from the current SoP charts suggested by Youd et al. 2001 and Idriss and Boulanger 2008 are also listed in Table 2. These charts provide $K_\sigma = 0.5 - 0.7$ and $0.7 - 0.85$ at 6 atm for loose and dense sand, respectively.

It is noteworthy that the values obtained from the centrifuge are greater than 1.0, with the cyclic resistance ratio increasing rather than decreasing as the overburden pressure increases from 1 to 6 atm. The centrifuge results led to significantly higher correction factors compared to the state-of-practice values in the literature based on undrained cyclic tests. These high field K_σ values at 6 atm in the centrifuge are most probably related to the more significant partial drainage in the 6-atm experiments compared with the 1-atm experiments. The high K_σ values obtained from centrifuge testing, as well as the possible general validity of this trend for other sands, are investigated in some depth in Abdoun et al. (2020).

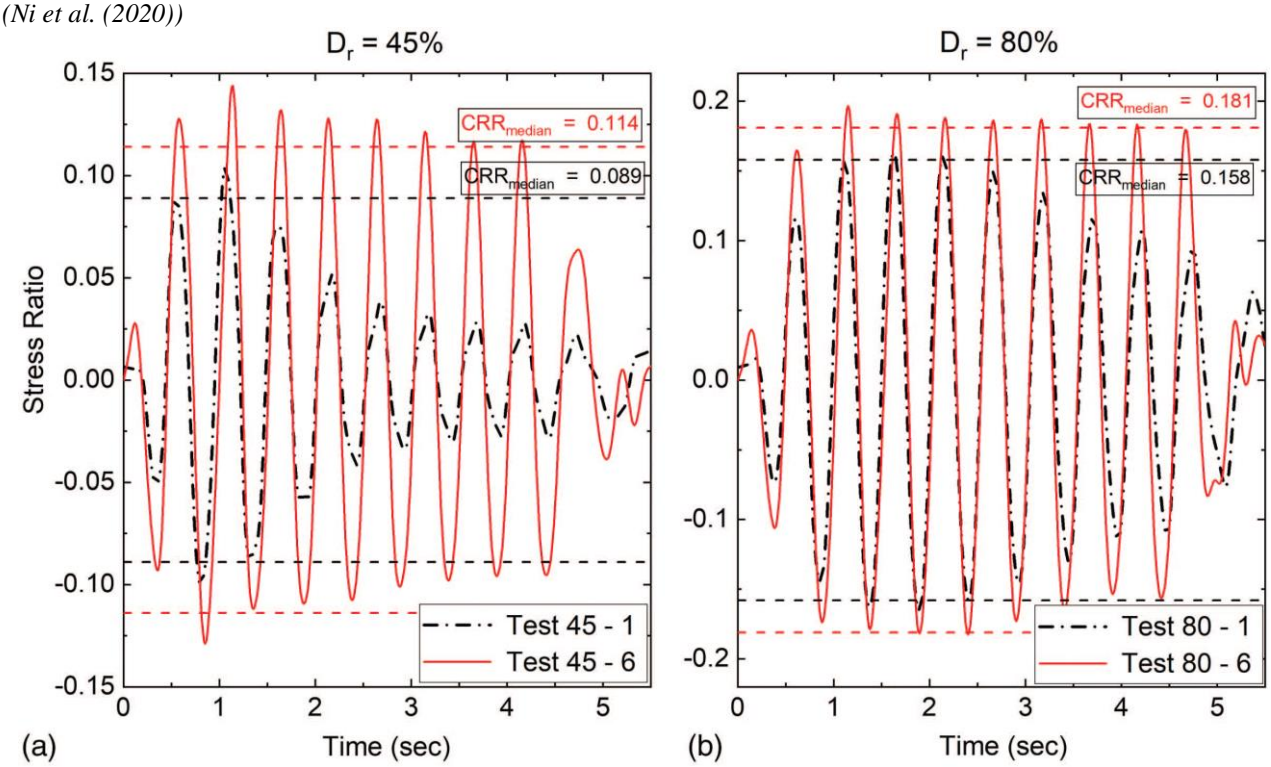

Figure 3: Time histories of shear stress ratio and representative CSR values for bottom elevations within the sand layer for (a) Tests 45-1 and 45-6; and (b) Tests 80-1 and 80-6. (Abdoun et al. (2020))

Table 2: Overburden Pressure Correction Factor (K_σ)

Experiment	$(r_u)_{max}$	Field K_σ (Obtained from Centrifuge)	State-of-Practice (Laboratory undrained $\boldsymbol{K_\sigma}$)	
			K_σ proposed by Youd et al. (2001)	K_σ proposed by Idriss and Boulanger (2008)
Test 45-1	0.80	1.28	0.7	0.85
Test 45-6	0.76			
Test 80-1	0.92	>1.15	0.5	0.7
Test 80-6	0.60			
Test 45-1 (DD)	0.68	<1.30	0.7	0.85
Test 45-6 (DD)	0.85			

4 CONCLUSIONS

The results for six centrifuge tests were used to investigate the behaviour of clean Ottawa sand, focusing on assessing how field drainage conditions influence the overburden pressure correction factor K_σ. These experiments encompassed four tests that explored the impact of single drainage conditions at two distinct relative densities (loose and dense soil configurations). Additionally, the effect of double drainage conditions was investigated under loose soil scenarios.

The findings from these studies have demonstrated that the currently accepted K_σ values used in the field are more conservative and do not fully account for variations in drainage conditions that may differ from laboratory settings. As such, updated K_σ values were proposed for single and double drainage scenarios. These values aim to more accurately reflect real-world conditions and should be considered for implementation in future geotechnical engineering projects.

ACKNOWLEDGEMENTS

The authors wish to thank the RPI geotechnical centrifuge technical staff for their help in the project and the preparation of this paper. The research was supported by the National Science Foundation under Grant No. 1545026 and 1904313, and by NYU Abu Dhabi; this support is gratefully acknowledged. This work was partially supported by the Sand Hazards and opportunities for Resilience, Energy, and Sustainability (SHORES) Center, funded by Tamkeen under the NYUAD Research Institute Award CG013.

REFERENCES

Abdoun, T. et al., 2020. Pore Pressure and Kσ Evaluation at High Overburden Pressure under Field Drainage Conditions. II: Additional Interpretation. *Journal of Geotechnical and Geoenvironmental Engineering, 146(9), pp. 04020089-1-16.*

Boulanger, R. W., 2003. High Overburden Stress Effects in Liquefaction Analyses. *Journal of Geotehcnical and Geoenvironmental Engineering, ASCE, pp. 1071-1082.*

Boulanger, R. W. and Idriss, I. M., 2004. State Normalization of Penetration Resistance and the Effect of Overburden Stress on Liquefaction Resistance. *California, s.n.*

Dobry, R. and Abdoun, T., 2015. Cyclic Shear Strain Needed for Liquefaction Triggering and Assessment of Overburden Pressure Factor Ks. *Journal of Geotechnical and Geoenvironmental Engineering, ASCE, pp. 04015047-1-18.*

Elgamal, A. W., Zeghal, M., Taboada, V., & Dobry, R. (1996). Analysis of site liquefaction and lateral spreading using centrifuge testing records. *Soils and Foundations, 36(2), 111 - 121.*

Elgamal, A. W., Zeghal, M., Tang, H. T., & Stepp, J. C. (1995). Lotung Downhole Array. I: Evaluation of Site Dynamic Properties. *Journal of Geotechnical Engineering, 121(4), 350 - 362.*

Gillette, D., 2013. Liquefaction issues for dam safety—Bureau of Reclamation, *Washington, DC: National Research Council of the National Academies.*

Harder, L. F. J., 1988. Use of penetration tests to determine the cyclic loading resistance of gravelly soils during earthquake shaking, *s.l.: Ph.D. thesis, Dept. of Civil Engineering, Univ. of California.*

Hynes, M. E. and Olsen, R. S., 1999. Influence of Confining Stress on Liquefaction Resistance. *Baltimore, Maryland, s.n., pp. 10-11.*

Idriss, I. M. and Boulanger, R. W., 2008. Soil Liqefaction during Earthquakes, *Oakland, CA: Monograph MNO-12, Earthquake Engineering Resarch Institute.*

Montgomery, J., Boulanger, R. W. and Harder, L. F. J., 2012. Examination of the Kσ overburden correction factor on liquefaction resistance, *Davis, CA: UCD/CGM-12-02, Center for Geotehcnical Modeling, Departmenet of Civil and Environmental Engineering, University of California.*

Ni, M., Abdoun, T., Dobry, R. and El-Sekelly, W., 2021. Effect of Field Drainage on Seismic Pore Pressure Buildup and Kσ under High Overburden Pressure. *Journal of Geotechnical and Geoenvironmental Engineering, pp. 04021088-1-15.*

Ni, M. et al., 2020. Pore Pressure and Kσ Evaluation at High Overburden Pressure under Field Drainage Conditions. I: Centrifuge Experiments. *Journal of Geotechnical and*

Geoenvironmental Engineering, 149(9), pp. 04020088-1-14.

Seed, H. B., 1983. Earthquake-resistant design of earth dams.. *Philadelphia, ASCE.*

Seed, R. B. and Harder, L. F. J., 1990. SPT-based Analysis of Cyclic Pore Pressure Generation and Undrained Residual Strength, *Berkeley, California: Proc. H. Bolton Seed Memorial Symposium, University of California.*

Seed, H. B., & Idriss, I. M. (1971). Simplified Procedure for Evaluation Soil Liquefaction Potential. *Journal of the Soil Mechanics and Foundations Division, ASCE, 1249-1273.*

Vaid, Y. P. and Sivathayalan, S., 1996. Static and cyclic liquefaction potential of Fraser Delta sand in simple shear and triaxial tests.. *Can. Geotech., p. 281–289.*

Vaid, Y. P. and Thomas, J., 1995. Liquefaction and Post-Liquefaction Behavior Sand. *Journal of Geotechnical Engineering, ASCE, pp. 163-173.*

Youd, T. L. et al., 2001. Liquefaction Resistance of Soils: Summary Report from the 1996 NCEER and 1998 NCEER/NSF Workshops on Evaluation of Liquefaction Resistance of Soils. *Journal of Geotechnical and Geoenviromental Engineering, ASCE, pp. 817-833.*

Zeghal, M., Elgamal, A. W., Tang, H. T., & Stepp, J. C. (1995). Lotung Downhole Array. II: Evaluation of Soil Nonlinear Properties. *Journal of Geotechnical Engineering, 121(4), 363 - 378.*